

Creep Viscosity and Stress Relaxation of Gel-Derived Silicon Oxycarbide Glasses

Tanguy Rouxel^{*,†}

Laboratoire de Mécanique Appliquée de l'Université de Rennes 1 (LARMAUR), UPRES-JE 2310, Université de Rennes 1, Campus de Beaulieu, 35042 Rennes Cedex, France

Gian-Domenico Soraru^{*}

Dipartimento di Ingegneria dei Materiali, Università di Trento, 38050 Trento, Italy

Jean Vicens

LERMAT, ISMRA, FRE-CNRS 2149, 14050 Caen Cedex, France

The temperature dependence of the viscosity and stress-relaxation kinetics of sol–gel-derived SiOC glasses that contain up to 14 at.% carbon have been characterized in the temperature range of 1000–1400°C. The viscosity, as determined from relaxation experiments, is in good agreement with the creep viscosity and is typically two orders of magnitude higher than the viscosity of vitreous silica. However, materials suffer from partial crystallization at >1150°C, and the precipitation of β-SiC nanocrystals induces a flow-hardening behavior and results in a dynamic increase in viscosity, especially at >1200°C and for glasses with a high carbon content.

I. Introduction

THE mechanical properties, and refractoriness, of a glass are strongly dependent on the atomic bond strength and the degree of polymerization (crosslinking) in the atomic network. Indeed, remarkable improvement in the elastic moduli, hardness, fracture resistance, and fracture toughness is observed when trivalent nitrogen (N^{3+}) ions substitute for divalent oxygen (O^{2-}) ions in silicate glasses.^{1,2} For instance, the replacement of one in five O^{2-} anions increases the elastic moduli by 30% and the viscosity coefficient by two orders of magnitude at a given temperature (or a 50°C shift for a given viscosity).³ These overwhelming changes clearly correlate with the increase in the average coordination number in the glass network.^{4,5} Quite recently, silicon oxycarbide (SiOC) glasses were synthesized successfully using sol–gel methods.^{6,7} In such glasses, there is approximately one C atom per three Si atoms; in addition, ²⁹Si magic angle spinning–nuclear magnetic resonance (²⁹Si MAS-NMR) has shown that most of the C atoms get into $C(Si)_4$ four-fold coordinated sites, although some of the carbon is present as free carbon domains, which gives the glasses a black color.^{8,9} These oxycarbide glasses exhibit remarkable mechanical properties at room temperature,¹⁰ and their transition range is estimated to be >1300°C.

Following a preliminary work on the high-temperature viscosity and elasticity of a sol–gel-derived oxycarbide glass that contained 12 at.% carbon,¹¹ the effect of carbon content on the viscosity, stress-relaxation kinetics, and microstructural changes that occur at

temperatures of >1200°C, as observed via X-ray diffractometry (XRD) and high-resolution transmission electron microscopy (HR-TEM), have been studied. These effects are reported in this paper.

II. Materials

As the degree of crosslinking of the network is increased, a rapid increase of the glass refractoriness follows, so that common melting techniques cannot be used anymore: at such temperatures, most of the carbon escapes from the melt through the volatilization of carbon monoxide (CO) gas.¹² The sol–gel route used in the present work already has been reported in detail.^{7–9} In its mainlines, a (D^H, T^H) gel (where D^H and T^H represent $HSiO_2$ and $HSiO_3$ units, respectively) first is synthesized from the polycondensation of a mixture of methyldiethoxysilane ($HMeSi(OEt)_2$) and triethoxysilane ($HSi(OEt)_3$). Then, the gel is pyrolyzed at a temperature of 1000°C, under inert atmosphere, to obtain a black glass that consists of (i) an oxycarbide phase, where carbon atoms form $C(Si)_4$ tetrahedra (the stoichiometric composition is written as $SiC_xO_{2(1-x)}$); (ii) free carbon microdomains; and eventually (iii) free silicon precipitates. This latter situation occurs when the D^H/T^H molar ratio is <0.5, whereas the free carbon content increases as the D^H/T^H molar ratio increases at >0.5. Let us note this ratio as y and the corresponding glass as D^HT^Hy . Two grades of glass were studied: $D^HT^H0.5$ and D^HT^H1 .

The number of C atoms in four-fold coordination to silicon and the free carbon content are key parameters to understand the properties of these glasses. The number of Si–C bonds can be estimated from the O/Si ratio in the gel, using the charge-balance equation, assuming that, in the oxycarbide phase, each C atom replaces two O atoms and no Si–Si nor C–O bonds form:

$$(C/Si)_{oxy} = \frac{2 - (O/Si)_{gel}}{2} \quad (1)$$

The O/Si ratio can be calculated from the D^H/T^H ratio, which can be given by the relation

$$(O/Si)_{gel} = \frac{y + \frac{3}{2}}{y + 1} \quad (2)$$

or is determined via chemical analysis. The difference between $(C/Si)_{gel}$ and $(C/Si)_{oxy}$ gives an estimation of the minimum amount of free carbon that remains in the glass. The $(C/Si)_{gel}$ ratio is given by the relation

$$(C/Si)_{gel} = \frac{y}{y + 1} \quad (3)$$

R. Raj—contributing editor

Manuscript No. 188548. Received May 23, 2000; approved November 13, 2000.

^{*}Member, American Ceramic Society.

[†]Author to whom correspondence should be addressed.

and the free carbon content (C_{free}) is expressed as

$$C_{\text{free}} = \frac{C_{\text{total}} - C_{\text{oxy}}}{C_{\text{total}}} \quad (4)$$

The results of the *ab initio* calculation are summarized in Table I, along with the results of the chemical analysis and some physical properties. The studied materials were pyrolyzed via treatment at 1000°C for 1 h, and they contained <1 wt% hydrogen (via chemical analysis).

Both D^HT^H0.5- and D^HT^H1-grade specimens contained some free carbon after firing, although the amount of free carbon was >10 times greater in the latter grade. A D^HT^H0.5-grade powder specimen was observed via HRTEM (Model 002B Topcon microscope, operating at 200 kV with a resolution of 0.18 nm). The material was dense, homogeneous, and almost completely amorphous. Very few isolated heterogeneities were visible; these features mainly consisted of turbostratic ribbonlike carbon domains (free carbon) <4 nm thick and silicon carbide (SiC) nuclei <3 nm in diameter (see Fig. 1). In any case, the volumetric percentage of free carbon was <3% and, hence, was assumed to have a minor effect on the mechanical behavior.

The oxycarbide glassy phases in both grades were very similar. Their theoretical stoichiometric compositions, as determined from simple charge-balance considerations, were SiC_{0.33}O_{1.33} and SiC_{0.375}O_{1.25} for the D^HT^H0.5 and D^HT^H1 grades, respectively. Accordingly, there should be little difference in the flow behavior, as will be discussed in the next section.

Oxycarbide-glass rods 20 mm long and 1.5 mm in diameter were obtained from gel rods after a pyrolysis treatment in flowing argon at 1000°C in a silica tube (for details, see the work of Soraru and co-workers^{8,9}). These rods later were used as test specimens in this study.

III. High-Temperature Flow Behavior

(I) Creep Viscosity

Three-point bending creep experiments (span length of 15 mm) were conducted under a pressure of 100 MPa in a nitrogen atmosphere (in a gas-tight chamber). The specimen deflection was recorded *in situ* via differential measurement, using a linear variable displacement transducer (LVDT) (for details, see Rouxel *et al.*¹³). Temperature jumps were conducted in the temperature range of 995°–1365°C. No creep was observed at <995°C. Results obtained on a D^HT^H1-grade specimen are plotted in Fig. 2. The creep curves exhibit relatively stationary flow stages as long as the temperature remains lower than 1150°C. From 1150°C to 1215°C, the creep rate continues to decrease during the testing. A soak time of 1 d was applied at 1215°C, to follow the creep-hardening

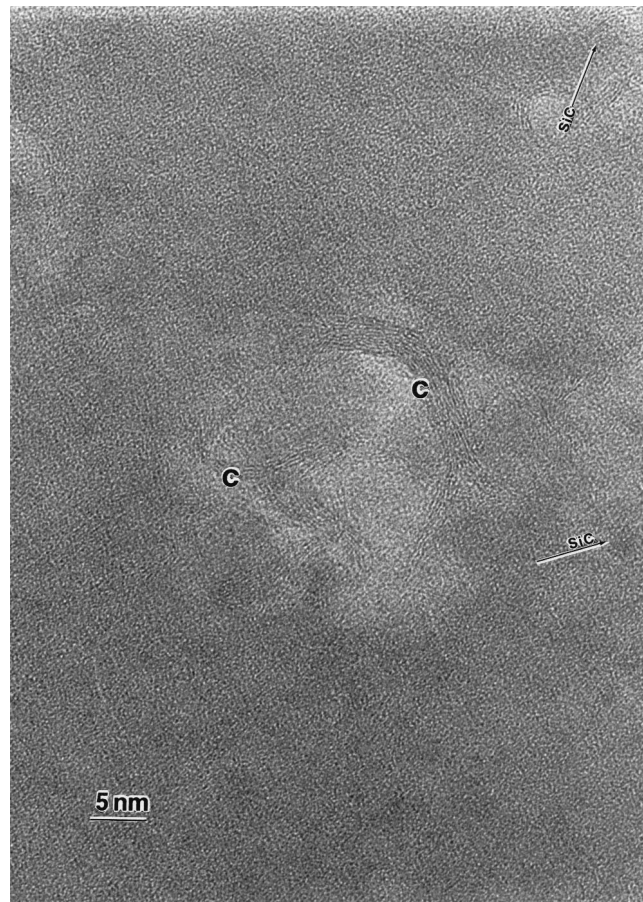


Fig. 1. HRTEM micrograph of an as-synthesized D^HT^H0.5-grade specimen. Turbostratic graphite units (ribbons) <4 nm thick are visible (marked by the letter “c”). Rare and hardly observable nuclei (presumably β-SiC) <3 nm in diameter also are present; these features are marked by arrows.

regime. Stationary creep rates again are observed after this treatment, at 1315° and 1365°C. It was previously reported^{11,14–16} that, in such glasses, crystallization starts at >1150°C and leads to the formation of β-SiC nanocrystals and, to a lesser extent, β-cristobalite (β-SiO₂) (reflections are observed at 2θ angles of 35°, 60°, and 72° in the XRD spectra of specimens that were heated to >1150°C). The average size of the crystallites, as estimated from the XRD spectra, after 12 h at 1200°C, was 2.5 nm. The crystallization process resulted in a composite microstructure

Table I. Glass Composition and Physical Properties of SiOC Glasses

| Property/characteristic | Value | | |
|-------------------------------------|-----------------------------|--|--|
| | SiO ₂ | D ^H T ^H 0.5 [†] | D ^H T ^H 1 [†] |
| Gel | | | |
| Atomic ratio | | | |
| O/Si | 2 | 1.33 (1.4) | 1.25 (1.4) |
| C/Si | 0 | 0.33 (0.35) | 0.5 (0.51) |
| Glass | | | |
| Chemical formula | SiO ₂ | SiC _{0.32} O _{1.39} | SiC _{0.47} O _{1.45} |
| (C/Si) _{oxy} | 0 | 0.335 (0.31) | 0.375 (0.28) |
| C _{free} , from Eq. (4) | 0.0 | 0.03 | 0.4 |
| Density, ρ | 2.20 g/cm ³ | 2.23 g/cm ³ | 2.20 g/cm ³ |
| Coefficient of thermal expansion, α | 0.57 × 10 ⁻⁶ /°C | 3.12 × 10 ⁻⁶ /°C | Not determined |
| Maximum stress, σ _{r,max} | Not determined | 750 MPa | 720 MPa |
| Mean stress, σ _{r,mean} | 60 MPa | 450 MPa | 450 MPa |
| Elastic modulus, E | 73 GPa | 104 ± 4 GPa | 110 ± 6 GPa |
| Hardness, H _V | 6.2 GPa | 7.7 ± 0.1 GPa | 8.3 ± 0.1 GPa |

[†]Data for D^HT^H glasses are taken from the work of Soraru and co-workers.^{9,10} Results of the chemical analyses are indicated in parentheses; Si, C, and H contents were analyzed by Service d'Analyse Elementaire du CNRS, France. Oxygen content was estimated using the difference.

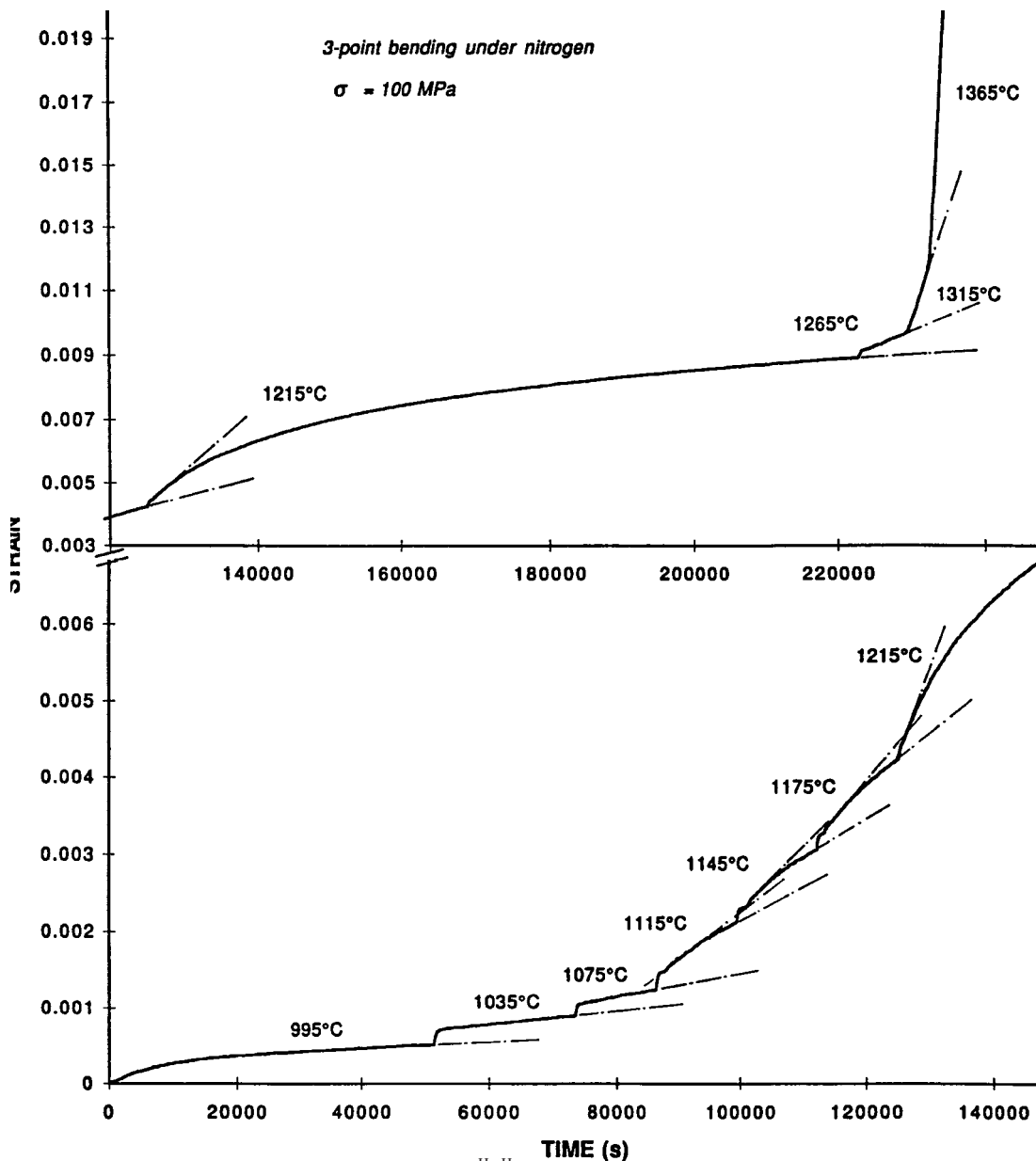


Fig. 2. Typical temperature-jump creep curve obtained in bending a $D^{HTH}1$ -grade specimen. Note that stationary flow stages are reached after a few hours at 1035° and 1075°C, whereas a long hardening stage is observed at 1215°C. The x- and y-axis origins of the portion of the curve recorded at $T > 1215^\circ\text{C}$ were shifted for the sake of clarity.

where β -SiC crystals were dispersed almost homogeneously, although some relatively large crystals (5–8 nm in diameter) were observed via HRTEM (Fig. 3). Heat treatment at 1300°C led to further enhancement of the crystallization. However, at 1300°C, an equilibrium composition is attained after 3 h, and no further changes are observed by heating at 1400°C.¹¹ This observation strongly suggests that crystallization was complete at 1300°C. Thus, at this stage, the hardening behavior, which is more pronounced in the case of the $D^{HTH}1$ -grade specimen, tentatively is related to the dynamic crystallization of the glass. This phenomenon will be discussed further in section IV.

The viscosity coefficient (η), hereafter referred as viscosity, was calculated from the strain rate ($\dot{\epsilon}$) versus stress (σ) data, based on a Newtonian flow behavior:

$$\eta = \frac{\sigma}{2(1 + \nu)\dot{\epsilon}} \quad (5)$$

where ν is Poisson's ratio. σ and $\dot{\epsilon}$, which are the flow stress during the pseudo-stationary creep stage and the corresponding strain rate, respectively, are given by the following relations:

$$\sigma = \frac{PS}{\pi R^3} \quad (6)$$

$$\dot{\epsilon} = \left(\frac{12R}{S^2}\right)\dot{u} \quad (7)$$

where P is the applied load, S the span length, R the specimen radius, and \dot{u} the deflection rate. The Poisson's ratio was assumed to be equal to 0.17 (which is that of silica glass, ν_{SiO_2}), and a stress of 100 MPa was applied to the specimen.

Viscosity curves are plotted in Fig. 4. Our data are in good agreement with those obtained by Renlund *et al.*¹⁷ and An *et al.*,¹⁸ whose data were for chemical-precursor-derived amorphous silicon oxycarbide and silicon carbonitride amorphous materials, respectively. Because of the strain hardening that was observed in the intermediate temperature range (1150°–1215°C), the value of η increases during testing at these temperatures, as illustrated by the arrows on the curve that corresponds to the $D^{HTH}1$ -grade specimen. In this temperature range, crystallization produces a glass-matrix particulate composite and affects the flow kinetics,

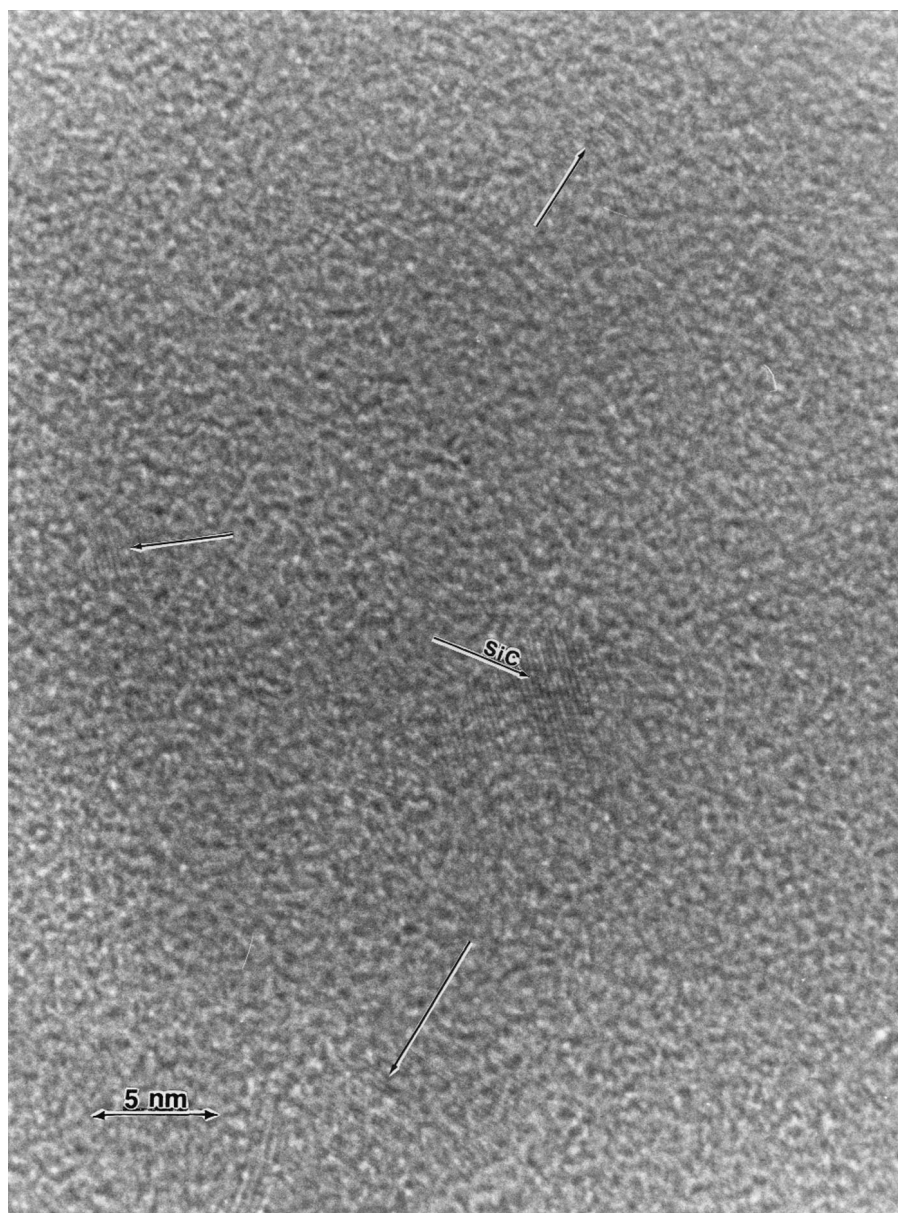


Fig. 3. HRTEM micrograph of a D^HT^H1-grade specimen after creep testing, following the temperature-jump procedure illustrated in Fig. 2. Many small β -SiC crystallites, a few nanometers in size, are visible (marked by arrows). A large β -SiC precipitate 7 nm in size also is observed ([110] zone axis).

especially for the D^HT^H1-grade specimen. In the case of the D^HT^H0.5-grade specimen, the volume fraction of SiC is probably not large enough to have a noticeable effect on the viscous flow. Moreover, the presence of SiC results in a tendency for the activation energy for flow to be higher at $>1200^\circ\text{C}$, approaching the value for a pure silica glass with low hydroxyl content.¹⁹ Hence, it is likely that this change reflects the decrease of the carbon content in the residual glass that follows crystallization. In the temperature range that corresponds to the glass transition of vitreous silica ($T_g \approx 1190^\circ\text{C}$), the viscosity of the oxycarbide glass is still very high ($>10^{14}$ Pa·s). Furthermore, the difference between the data from the SiOC glasses and those of fused silica increases as the temperature increases, and the apparent activation energy for flow is much smaller for the oxycarbide glasses ($\Delta G_a = 296$ kJ/mol)¹¹ than for silica ($\Delta G_a \approx 500$ – 700 kJ/mol), regardless of the hydroxyl content (up to 0.12 wt%). A transition temperature of 1350°C is determined by extrapolating the viscosity curve of the D^HT^H0.5 glass to the conventional viscosity range of 10^{12} – $10^{12.6}$ Pa·s that is associated with the transition.

(2) Stress Relaxation

Stress-relaxation experiments were conducted during bending in a gas-tight chamber under a nitrogen atmosphere, by enslaving

the actuator during the relaxation experiments to keep the specimen position constant. It must be emphasized that the *specimen deformation is much smaller than the actuator displacement*, especially at relatively low temperature, when the specimen deforms little while attainment of the thermal equilibrium of the entire equipment requires a long time. Approximately 2000 points were recorded for a single experiment. Such a large population of (stress,time) points is required to model the behavior, especially during the early times of the relaxation stage, when the relaxation kinetics are very fast. The heating and cooling rates each were $10^\circ\text{C}/\text{min}$. Rapid loading (using a cross-head speed of 0.5 mm/min) up to an initial stress (σ_0) of 100 MPa was performed. The experimental results are plotted in Fig. 5 and reported in Table II. Because of crystallization, the relaxation is slower at 1240°C than at 1200°C , and the curves that are obtained at $>1200^\circ\text{C}$ must be understood to be those of a glass-matrix particulate composite. The relaxation kinetics could be remarkably well modeled by the so-called Kohlrausch–Williams–Watt (KWW) equation that is quoted often in glass science:²⁰

$$\phi(t) = \exp\left[-\left(\frac{t}{\tau}\right)^b\right] \quad (8)$$

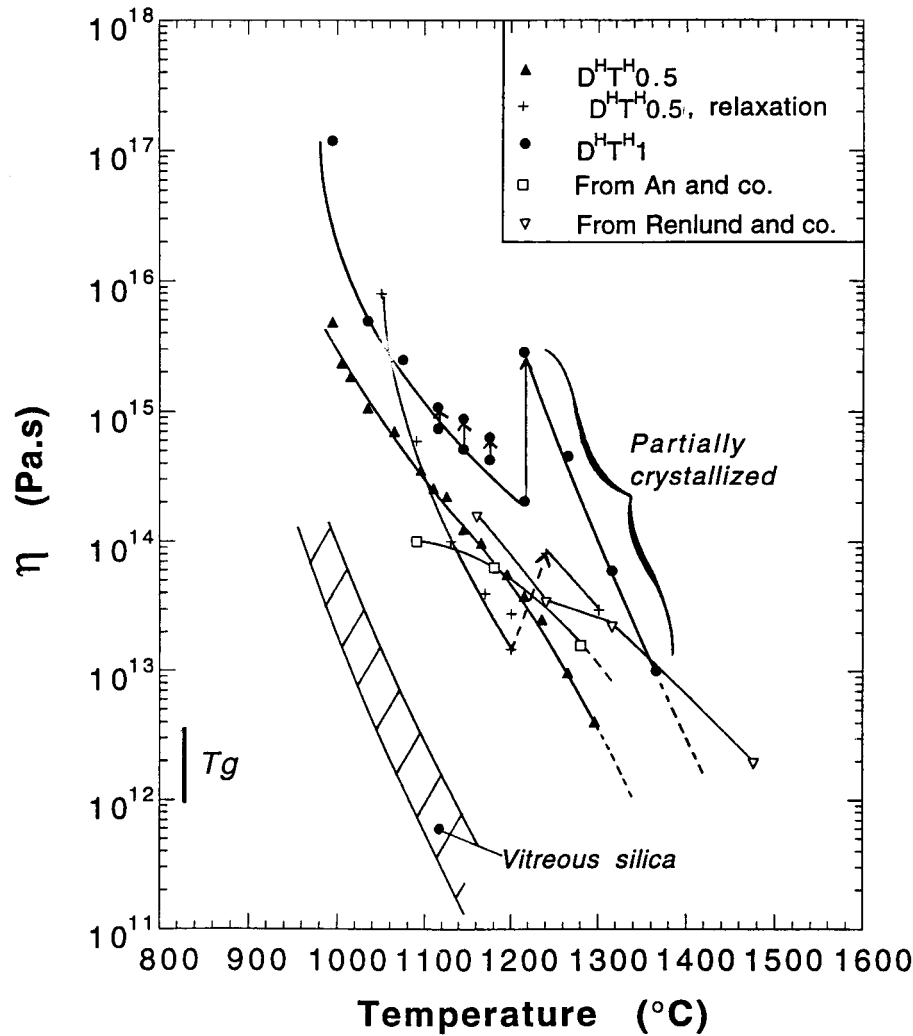


Fig. 4. Temperature dependence of the viscosity η of silicon oxycarbide glasses. Arrows indicate ranges where dynamic crystallization occurs to form β -SiC and, to a lesser extent, β -SiO₂ precipitates. Data concerning vitreous silica are reprinted from Hetherington *et al.*¹⁹

where τ is the characteristic relaxation time. (One must recall that $\phi(t)$ is defined as $\phi(t) = \sigma(t)/\sigma_0$.) Following previous works,^{21,22} the parameter b is called the correlation factor and can be related tentatively to the mobility of a structural unit at the atomic or molecular scale. The value of b ranges from 0 (which indicates strong intermolecular coupling, allowing for pure elastic deformation only) to 1 (which indicates weak correlation, corresponding to the simple Debye–Maxwell relaxation of liquids). Following the theory of thermally activated deformation, τ can be regarded as the waiting time of the activation process, and, according to an Arrhenian dependence, an activation energy of 617 kJ/mol was determined from the data of Table II below the temperature range for crystallization. This value is close to that reported for the viscous flow of vitreous silica; therefore, relaxation is suggested to occur via viscous flow of the oxygen-rich region through channels that exist between the relatively rigid carbon-rich units. The value of η can be estimated from the τ values, using the Boltzmann superposition principle:²³

$$\eta = \mu \int_0^{\infty} \phi(t) dt \quad (9)$$

where μ is the shear modulus.

In the present case, where the KWW relationship is valid, the relaxation function can be integrated readily and the former expression can be rewritten as

$$\eta = \left(\frac{\mu}{b}\right) \tau \Gamma\left(\frac{1}{b}\right) \quad (10)$$

where Γ is the gamma function. Values of η that have been obtained this way—using the experimental data for μ from Rouxel *et al.*¹¹—are summarized in Table II. (Note that, similar to vitreous silica, the oxycarbide glass exhibits the astonishing ability to become stiffer and stiffer with increasing temperature!) The viscosity for the D^HT^H0.5-grade specimen, relative to temperature, is plotted in Fig. 4. These values fall in the range that is determined by creep, and, again, the crystallization of finely distributed β -SiC and β -SiO₂ crystals leads to an increase in the value of η at temperatures in the range of 1200°–1250°C.

IV. Discussion

The results described in the previous section show that the introduction of carbon that is covalently bonded to silicon provides a significant increase in η , and most data that have been reported so far on glasses that contain 10–20 at.% carbon are consistent with an ~ 2 -orders-of-magnitude shift, in comparison with vitreous silica, and result in transition ranges that cannot be attained without crystallization and are virtually located at 1300°–1400°C. In this section, we will try to obtain insight into the effect of crystallization on the flow behavior.

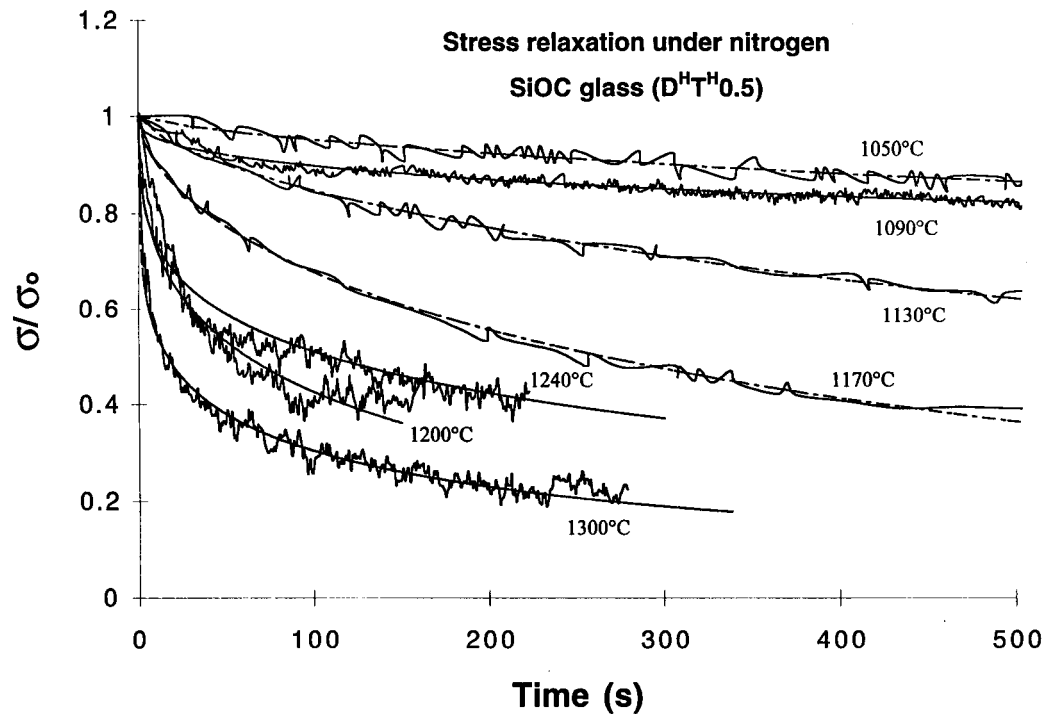


Fig. 5. Stress-relaxation curves obtained in bending a $D^{HT}1$ -grade specimen with an initial stress σ_0 of 100 MPa. Curvefitting was performed using the KWW equation (Eq. (8)).

Table II. Stress-Relaxation Characteristics of $D^{HT}0.5$ Silicon Oxycarbide Glass

| Temperature (°C) | Shear modulus, μ (GPa) | Relaxation time, τ (s) | Parameter b , from Eq. (8) | Gamma function, $\Gamma(1/b)$ | Viscosity, η (Pas) |
|------------------|----------------------------|-----------------------------|------------------------------|-------------------------------|-------------------------|
| 1050 | 46.7 | 41132 | 0.37 | 1.54 | 7.99×10^{15} |
| 1090 | 47.1 | 9378 | 0.66 | 0.89 | 5.93×10^{14} |
| 1130 | 48.0 | 1552 | 0.66 | 0.89 | 1.00×10^{14} |
| 1170 | 49.4 | 491 | 0.59 | 0.97 | 3.97×10^{13} |
| 1200 | 50.4 | 129 | 0.47 | 1.06 | 1.47×10^{13} |
| 1240 | 52.76 | 306 | 0.35 | 1.67 | 8.14×10^{13} |
| 1300 | 57.53 | 55.5 | 0.30 | 2.77 | 2.95×10^{13} |

The maximum volume fraction of SiC can be calculated from the stoichiometric formula of the oxycarbide glass phases, assuming that all the carbon of the oxycarbide phase gets into SiC particles, with the free carbon reacting preferentially with oxygen. Volume fractions of 17.2 and 19.9 vol% SiC particles are estimated this way for the $D^{HT}0.5$ - and $D^{HT}1$ -grade specimens, respectively. Attempts to predict the shear viscosity of glass-matrix particulate composites have created several models over the past twenty years. In most cases, the models start from constitutive equations that are derived from known elasticity solutions and transpose these solutions to the case of viscoelasticity, using the analogy between pure Hookean elasticity and pure Newtonian flow. It follows that displacements are reinterpreted as velocities and the correspondence between the shear modulus μ and the viscosity coefficient η is expressed by the relation $\mu_c/\mu = \eta_c/\eta$, where the subscript "c" refers to the composite.

The solution for the effective shear modulus of a dilute medium of elastic spherical particles in a continuous phase of another material can be found in several textbooks. Using a simple composite spheres model,²⁴ and considering a second-phase volume fraction of 20% (with $\mu = 180$ GPa and $\nu = 0.17$ for SiC), one can obtain the following relations: $\mu_c = 1.23\mu$, or $\eta_c = 1.23\eta$. As also noted by An *et al.*,¹⁸ this increase is much less than that observed experimentally, which, in the present case at 1215°C for the $D^{HT}1$ -grade specimen, reaches a factor of 14. However, in contrast to the conclusions by An *et al.*,¹⁸ in the present case, the

increase in η clearly is related to the partial crystallization of the glass to form β -SiC precipitates in carbon-rich regions. Furthermore, such a discrepancy already has been observed in SiC-particle-reinforced oxynitride glass, which is a rather similar material.^{25,26} In this case, the rapid increase in η for second-phase volume fractions of $>10\%$ was discussed, relative to the effect of particle size, which, of course, is not considered in elasticity schemes that are based on continuum mechanics. For a given volume fraction, the value of η increases rapidly as the particle size decreases.²⁶ For instance, for particulate composites that contain 28 vol% SiC, η_c/η has values of 3.68, 4.45, and 10.6 for particle sizes of 31, 13, and 3 μm , respectively. In regard to these data, a value of $\eta_c/\eta = 14$ for a glass-matrix composite with 20 vol% SiC particles that are 2.5 nm in diameter (i.e., in a material similar to $D^{HT}1$) at $>1200^\circ\text{C}$ seems realistic.

Deviation from the model might have different sources. First of all, the non-shape-conservative nature of flow makes the use of the elasticity-viscosity analogy questionable, especially for large elongations, when changes in the interparticle distances, relative to a growing number of inclusion-inclusion contacts and eventually agglomerates formation, are involved. These latter phenomena increase the viscosity and lead to strain hardening, i.e., a strain-(or time-)dependent viscosity. Second, models have been developed essentially for spherical inclusions, independent of the inclusion size. It is well recognized that the particle morphology and size are the most-important variables, relative to suspension rheology.

Indeed, a small particle size usually results in a high viscosity, and the smaller the size, the lower the percolation and rigidity thresholds. Previous reports have shown that the increase in the crystallized fraction that result from the increase of the soaking temperature does not induce a change in the size of the β -SiC nanocrystals.¹¹ Therefore, crystallization proceeds through a growing number of small β -SiC crystals. The interparticle distance can be estimated from the average size and volume fraction of the particles. For instance, the following expression was proposed by Fullman²⁷ for the mean free path (Δ) between the surfaces of spherical particles of uniform diameter D that have been distributed statistically throughout a matrix:

$$\Delta = \frac{2D(1 - f_p)}{3f_p} \quad (11)$$

where f_p is the volume fraction of particles. Values of $D = 2.5$ nm and $f_p = 0.2$ yield a mean free path of $\Delta = 6.7$ nm. Note that this value of Δ compares well with the distances that are observed in Fig. 3. In fact, Δ is only one order of magnitude larger than the typical ring size in amorphous silica: the size of a five-fold ring (which also is called a cyclopentasiloxane structure) is ~ 0.5 nm. Furthermore, the effective flow channels between the SiC particles might be significantly smaller, because of the presence of relatively rigid layers around the particles. These layers consist of $\text{Si}_x\text{O}_{4-x}$ units that act as bridges between the SiC particles and the SiO_2 matrix.

V. Conclusion

The viscosity coefficient and stress-relaxation kinetics of gel-derived silicon oxycarbide glasses with different carbon contents were characterized in the temperature range of 1000°–1400°C. The viscosity was ~ 2 orders of magnitude higher for silicon oxycarbide glasses than for vitreous silica, and the higher the carbon content, the higher the viscosity. Crystallization occurred at $>1150^\circ\text{C}$ and resulted in the precipitation of large (2–3 nm) β -SiC crystallites (which could be observed via high-resolution transmission electron microscopy) and, to a lesser extent, β - SiO_2 . This crystallization process induced a dynamic increase in the viscosity, especially in the D^{HTH} -grade glass specimen, which contained ~ 14 at.% carbon, and impeded the experimental determination of the glass-transition range, which would be otherwise expected to be observed at 1350°–1400°C, according to extrapolation of the viscosity curves.

Acknowledgments

Most of the experiments were conducted during the stay of author TR at ENSCI (Limoges, France). S. Testu (ENSCI) is greatly acknowledged for conducting the relaxation experiments.

References

- S. Hampshire, R. A. L. Drew, and K. H. Jack, "Viscosities, Glass Transition Temperatures, and Microhardness of Y-Si-Al-O-N Glasses," *J. Am. Ceram. Soc.*, **67** [3] C-46–C-47 (1984).
- D. R. Messier, "Preparation and Properties of Y-Si-Al-O-N Glasses," *Int. J. High Technol. Ceram.*, **3**, 33–41 (1987).
- T. Rouxel, M. Huger, and J. L. Besson, "Rheological Properties of Y-Si-Al-O-N Glasses—Elastic Moduli, Viscosity and Creep," *J. Mater. Sci.*, **27**, 279–84 (1992).
- R. K. Brow and C. G. Pantano, "Nitrogen Coordination in Oxynitride Glasses," *J. Am. Ceram. Soc.*, **67** [4] C-72–C-74 (1984).
- T. Rouxel, J. L. Besson, E. Rzepka, and P. Goursat, "Raman Spectra of SiYAlON Glasses and Ceramics," *J. Non-Cryst. Solids*, **122**, 298–304 (1990).
- H. Zhang and C. G. Pantano, "Synthesis and Characterization of Silicon Oxycarbide Glasses," *J. Am. Ceram. Soc.*, **73** [4] 958–63 (1990).
- F. Babonneau, G. D. Soraru, G. D'Andrea, S. Dire, and L. Bois, "Silicon Oxycarbide Glasses from Sol-Gel Precursors," *Mater. Res. Soc. Symp. Proc.*, **271**, 789–94 (1992).
- G. D. Soraru, "Silicon Oxycarbide Glasses from Gels," *J. Sol-Gel Science Technol.*, **2**, 843–48 (1994).
- G. D. Soraru, G. D'Andrea, R. Camprotrini, and F. Babonneau, "Si-O-C Glasses from Gels"; pp. 135–46 in *Ceramic Transactions*, Vol. 55, *Sol-Gel Science and Technology*. Edited by E. J. A. Pope, S. Sakka, and L. C. Klein. American Ceramic Society, Westerville, OH, 1995.
- G. D. Soraru, E. Dallapiccola, and G. D'Andrea, "Mechanical Characterization of Sol-Gel-Derived Silicon Oxycarbide Glasses," *J. Am. Ceram. Soc.*, **79** [8] 2074–80 (1996).
- T. Rouxel, G. Massouras, and G. D. Soraru, "High Temperature Behavior of a Gel-Derived SiOC Glass: Elasticity and Viscosity," *J. Sol-Gel Sci. Technol.*, **14**, 87–94 (1999).
- J. Homeny, G. G. Nelson, and S. H. Risbud, "Oxycarbide Glasses in the Mg-Al-Si-O-C System," *J. Am. Ceram. Soc.*, **71** [5] 386–90 (1988).
- T. Rouxel, F. Rossignol, J. L. Besson, P. Goursat, J. F. Goujaud, and P. Lespade, "Superplastic Deformation of a Monolithic Silicon Nitride"; pp. 351–58 in *Plastic Deformation of Ceramics*. Edited by J. Routbort, R. C. Bradt, and C. Brookes. Plenum Press, New York and London, U.K., 1995.
- G. D. Soraru and D. Suttor, "High Temperature Stability of Sol-Gel-Derived SiOC Glasses," *J. Sol-Gel Sci. Technol.*, **14**, 69–74 (1999).
- C. G. Pantano, A. K. Singh, and H. Zhang, "Silicon Oxycarbide Glasses," *J. Sol-Gel Sci. Technol.*, **14**, 7–25 (1999).
- K. Kamiya, A. Katayama, H. Suzuki, K. Nishida, T. Hashimoto, J. Matsuoka, and H. Nasu, "Preparation of Silicon Oxycarbide Glass Fibers by Sol-Gel Method: Effect of Starting Sol Composition on Tensile Strength of Fibers," *J. Sol-Gel Sci. Technol.*, **14**, 95–102 (1999).
- G. M. Renlund, S. Prochazka, and R. H. Doremus, "Silicon Oxycarbide Glasses: Part II. Structure and Properties," *J. Mater. Res.*, **6** [12] 2723–34 (1991).
- L. An, R. Riedel, C. Konetschny, H. J. Kleebe, and R. Raj, "Newtonian Viscosity of Amorphous Silicon Carbonitride at High Temperature," *J. Am. Ceram. Soc.*, **81** [5] 1349–52 (1998).
- G. Hetherington, K. H. Jack, and J. C. Kennedy, "The Viscosity of Vitreous Silica," *Phys. Chem. Glasses*, **5** [5] 130–36 (1964).
- See, for example, F. L. Cumbra, F. Sanchez-Bajo, F. Guiberteau, J. D. Solier, and A. Munoz, "The Williams–Watts Dependence as a Common Phenomenological Approach to Relaxation Processes in Condensed Matter," *J. Mater. Sci.*, **28**, 5387–96 (1993). (Also see Ref. 23.)
- K. L. Ngai, A. K. Rajagopal, and S. Teitler, "Slowing Down of Relaxation in a Complex System by Constraint Dynamics," *J. Chem. Phys.*, **88**, 5086–94 (1988).
- J. Perez, J. Y. Cavallé, S. Etienne, and C. Jourdan, "Physical Interpretation of the Rheological Behavior of Amorphous Polymers through the Glass Transition," *Rev. Phys. Appl.*, **23**, 125–35 (1988).
- A. K. Varshneya (ed.), *Fundamentals of Inorganic Glasses*. Academic Press, Boston, MA, San Diego, CA, New York, and London, U.K., 1994.
- R. M. Christensen, "A Critical Evaluation for a Class of Micromechanics Models," *J. Mech. Phys. Solids*, **38**, 379–404 (1990).
- T. Rouxel and P. Verdier, "SiC Particle Reinforced Oxynitride Glass and Glass-Ceramic Composites: Crystallization and Viscoplastic Forming Ranges," *Acta Metall. Mater.*, **44** [6] 2217–25 (1996).
- T. Rouxel, B. Baron, P. Verdier, and T. Sakuma, "SiC Particle Reinforced Oxynitride Glass: Stress Relaxation, Creep and Strain-Rate Imposed Experiments," *Acta Mater.*, **46**, 6115–30 (1998).
- R. L. Fullman, "Measurement of Particle Sizes in Opaque Bodies," *Trans. AIME*, **197**, 447–52 (1953). □